

Quasi-continuous reconnection accompanied by FTEs during IMF $B_z \approx 0$ nT observed by Double Star TC-1 at the dawnside magnetopause

Guang Qing Yan^{1,2}, Forrest S. Mozer², Tai Phan², Chao Shen¹, Tao Chen¹, Yulia V. Bogdanova³, Henri Rème^{4,5}, Chris Carr⁶, Zhen Xing Liu¹

¹ State Key Laboratory of Space Weather, National Space Science Center, Chinese Academy of Sciences, Beijing, 100190, China;

² Space Science Laboratory, University of California, Berkeley, California 94720, United States of America;

³ RAL Space, Rutherford Appleton Laboratory, STFC, Harwell Oxford, Didcot, Oxfordshire, OX11 0QX, UK

⁴ IRAP, University of Toulouse, UPS-OMP, Toulouse, France;

⁵ CNRS, IRAP, 9 Ave. Colonel Roche, BP 44346, F-31028 Toulouse cedex 4, France;

⁶ The Blackett Laboratory, Imperial College London, Exhibition Road, London SW7 2AZ, United Kingdom

Corresponding author: Guang Qing Yan, Email: gqyan@spaceweather.ac.cn

Abstract: During a one-hour interval of interplanetary magnetic field (IMF) $B_z \approx 0$ nT, the equatorial spacecraft Double Star TC-1 encountered the dawn flank magnetopause many times at the magnetic local time (MLT) of about 08:00 and the latitude of about -27° . During each encounter, reconnection jets were observed with their velocities up to more than 500 km/s, significantly higher than the background flow in the magnetosheath. The fast flows match the theoretical prediction of Alfvénic acceleration well. The medium temperature and density of ions in the boundary layer indicate the open magnetic field topology inside this layer. The mainly southward and tailward flows of the plasma jets alongside with the negative slopes of the Walén test indicate that the spacecraft was located south of the reconnection site, consistent with both anti-parallel and component reconnection models. The accelerated flows were observed lasting for about one hour, with some modulations by the oscillations of the magnetopause, but no reversals in the direction of V_z were found during the interval. The significantly enhanced flows in the boundary layer compared to the adjacent magnetosheath indicate that the reconnection was quasi-continuously active at the magnetopause northward of the spacecraft under such IMF conditions. At the same time, the bipolar signatures in B_N with enhancements of the magnetic field indicate the occurrence of the Flux Transfer Events (FTEs). The observed reconnection was quasi-continuous, whereas the simultaneously accompanied FTEs were time-dependent under the IMF $B_z \approx 0$ nT. For this event, however, it is not possible to identify whether the reconnection was anti-parallel or component because the TC-1 was far away from the reconnection site.

Key words: continuous reconnection; flank magnetopause; Flux Transfer Event

1 Introduction

Magnetic reconnection is one of the most important processes of the solar wind-magnetosphere interaction, and plays a crucial role in the solar wind plasma transport into the magnetosphere. Dungey (1961, 1963) was the first to introduce the concept of reconnection into the solar wind-magnetosphere interaction and he developed models for reconnection at low latitude on the dayside magnetopause under southward IMF, and at high latitude on the magnetopause behind one or both cusps under northward IMF, respectively.

Reconnection may often happen when the field lines across the magnetopause are anti-parallel because of the short growth time of the tearing instability in the anti-parallel direction (Quest and Coroniti, 1978). The reconnection site could be deduced by the geometrical criteria of anti-parallel configuration (Crooker et al, 1979, Luhmann et al, 1984). Zong et al (2005) reported Cluster observations of reconnection at multiple X-lines at the edge of the northern cusp which were similar to the anti-parallel type. Dunlop et al (2009) investigated anti-parallel reconnection observed on the dayside closed field lines at the high latitude magnetopause.

On the other hand, both theoretical and observational analyses indicated that reconnection could still take place when the magnetic fields across the magnetopause are not anti-parallel, with the shear angle being much smaller than 180° (Cowley et al, 1973; Sonnerup et al, 1974). In this case the position of the reconnection line could be deduced by the geometrical criteria of the component reconnection model (Gonzales and Mozer, 1974). Chandler et al (1999) reported the component reconnection observed by Polar equatorward of southern cusp during northward IMF. Pu et al (2005, 2007) analyzed several events of component reconnection observed by TC-1 and Cluster near the sub-solar magnetopause. Kim et al (2002) also found evidence of component reconnection near the sub-solar point.

As a significant process that converts magnetic field energy into plasma energy, reconnection can be considered to be either steady (Paschmann et al, 1979; Gosling et al, 1982; Frey et al, 2003) or time-dependent, creating Flux Transfer Events, FTEs (Russell and Elphic, 1978, 1979), or quasi-periodic with some intermittency (Kan et al, 1988; Nishida et al, 1989). It is difficult to conclude whether steady or transient reconnection is more probable at the magnetopause. Phan et al (2000, 2001, and 2006) reported Equator-Geotail and Wind-Geotail observations of the extended reconnection at the flank magnetopause. Zheng et al (2005) investigated Cluster observations of continuous reconnection at the dayside magnetopause in the vicinity of the cusp. The global magneto-hydrodynamic (MHD) simulation by Raeder (2006) presented a generation mechanism of the intermittent FTEs in the form of repeated plasmoids that are independent of the external trigger.

Many observations of reconnection processes under northward IMF (Song et al, 1992; Chandler et al, 1999; Petrincic et al, 2000; Phan et al, 2003; Pu et al, 2005; Lavraud et al, 2002, 2005, 2006; Bogdanova et al., 2005, 2008; Øieroset et al, 2005; Yan et al, 2008) and southward IMF (Dunlop et al, 2005; Trattner et al, 2007; Yan et al, 2009) have been previously reported. The reconnection at the magnetopause was understood to be either stable or transient. Phan et al (2004) investigated observations of continuous reconnection by three Cluster spacecraft under steady IMF conditions, where the inner spacecraft observed the slowing of the accelerated flows while the outer one observed them more continuously. Rosenqvist et al (2008) analyzed the same event with the conclusion of continuous reconnection, but the reconnection rate could be modulated even under steady IMF. Hasegawa et al (2008) reported a quasi-continuous reconnection at the tailward of the cusp under northward IMF. However, there have been much fewer reports of continuous reconnection when IMF B_z was close to 0 nT.

In our observations, when IMF B_z was around 0 nT, the reconnection can be identified as a quasi-continuous process, as illustrated in Figure 6, whereas a series of the time-dependent FTEs were observed at the same time, showing the features of quasi-steadiness and time-dependence simultaneously.

The paper is organized as follows: Section 2 presents the details of the observation and its analysis. Section 3 gives a discussion of the event, and section 4 gives the summary of the presented work.

2 Observations

1
2
3
4 The Double Star Program (DSP) includes equatorial and polar orbiting spacecraft (Liu, 2005). The
5 Equatorial spacecraft TC-1 covered the dayside magnetopause region during spring, 2004. The instruments
6 onboard TC-1 measured magnetic field vectors, the ion temperature, bulk velocity and density, and the
7 electron temperature, bulk velocity and density. The data used in this work include the TC-1 magnetic field
8 measurements by the Flux Gate Magnetometer (FGM) (Carr et al., 2005), the ion parameters by the Hot Ion
9 Analyzer (HIA) (Rème et al., 2005), and the Flux Gate Magnetometer (FGM) (Balogh et al, 2001) on Cluster
10 SC1, as the IMF monitor in the upstream magnetosheath (Panel 1 in Figure 1). The time resolution used in this
11 work is the spin-resolution of 4 seconds, and the vectors are presented in the geocentric solar magnetospheric
12 (GSM) coordinates.
13

14
15 On May 2, 2004, TC-1 encountered the magnetopause many times at an MLT of about 8:00 and latitude of
16 about 27° (Figure 1), and crossed the magnetopause into the magnetosheath at about 18:47 UT, as identified
17 by the abrupt change in the observed B_z (Figure 2). The orbit of TC-1 was nearly tangential to the
18 magnetopause for several hours, as shown in Figure 1, which provided a good opportunity to observe the
19 magnetopause boundary layer and the processes at the magnetopause, such as reconnection. The northward
20 IMF lasted for about eight hours before the interval of interest, until it showed IMF $B_z \approx 0$ nT for about 2 hours.
21 Panel 1 in Figure 2 presents the IMF observed by SC1 of the Cluster in the upstream magnetosheath, at the
22 similar MLT as TC1. The time lag of 2 minutes has been counted in from the SC1 to TC1, because SC1 is
23 located 4 Re upstream of TC-1 in the X direction (Panel 1 in Figure 1). It can be seen that the draped IMF
24 B_z is very close to 0 nT, and the draped IMF B_y is the dominant component. The draped IMF B_x (green
25 line in Panel 1 of Figure 2) is smaller than the B_y (blue line in Panel 1 of Figure 2). The draped IMF
26 orientation observed by Cluster SC1 in the magnetosheath during this interval was found to be consistent
27 with the ACE observation, which is not shown. Because of the location at the flanks, the draping of the
28 magnetic field against the magnetopause plays a critical role in the orientation of the magnetosheath field.
29 At the location of SC1, about 4 Re upstream of TC-1, the observed draped IMF has significantly larger B_y
30 than B_x (both are negative). At the location of TC-1, the draped IMF observed in the magnetosheath has
31 the similar B_x (green line in Panel 5 of Figure 2) and B_y (blue line in Panel 5 of Figure 2), adjacent to the
32 magnetopause, shown in Panel 5 of Figure 2 (see 18:47 UT-19:06 UT). This rotation from dawnward at
33 SC1 to tailward at TC-1 is consistent with the draping effect in the magnetosheath at dawnside.
34

35 Under IMF $B_z \approx 0$ nT, during the nearly one-hour interval 17:55 UT-18:47 UT, the spacecraft observed
36 accelerated flows every time it encountered the magnetopause (Panel 4 in Figure 2). The velocity of the fast
37 flows, up to more than 500 km/s, was significantly higher than the background flow in the magnetosheath.
38 Such acceleration could likely be generated by reconnection, rather than from possible Kelvin-Helmholtz (K-H)
39 waves due to velocity shear or small penetrations at such a flank side of the magnetopause. The directions of
40 the flows were steadily southward ($-V_z$) and tailward ($-V_x$), also negative in the L-direction of the boundary
41 coordinates (the dominant and negative V_L in panel 7 of figure 2), implying the spacecraft was located
42 southward of the reconnection site. The accelerated flows were quite continuous, with some modulations
43 by
44 the magnetopause motion.

45 During the interval 17:55 UT-18:47 UT, the observed fast flows were always southward and tailward,
46 without any reversal. In fact, the fast flows were quite continuous during this interval because nearly 80% of
47 the time was filled by the high speed flows. It will also be discussed that the reconnection was quasi-
48 continuously active as shown in Figure 6. On the other hand, some bipolar signatures could be seen in B_N with
49 enhancements of the magnetic field (panel 5 and 6 of Figure 2), at 17:54 UT, 17:55 UT, 17:57 UT, 18:01 UT,
50 18:04 UT, 18:17 UT, 18:25 UT, 18:32 UT, 18:34 UT, 18:43 UT, 18:51 UT, and 18:54 UT, marked by the
51 vertical lines. The enhancements in the magnetic field occurred at every bipolar signature, indicating the
52 existence of the FTEs (e. g., Zhang, et al, 2010). The ion density increased at the FTEs (at 17:54 UT, 17:55 UT,
53 17:57 UT, 18:01 UT, 18:04 UT, 18:17 UT, 18:25 UT, 18:32 UT, 18:34 UT and 18:43 UT) inside the
54
55
56
57
58
59
60
61
62
63
64
65

1
2
3
4 magnetosphere while it decreased at the FTEs (at 18:51 UT and 18:54 UT) in the magnetosheath. This can be
5 understood in terms of the flux tubes that opened at the magnetopause between the magnetosheath and the
6 magnetosphere. Each FTE happened when the observed velocity increased or decreased which was caused by
7 the motion of the magnetopause.
8

9 In order to verify the occurrence of reconnection, the Walén tests have been carried out at the crossings of
10 the magnetopause current sheet. As illustrated in figure 3 (a~e, with the time intervals, correlations coefficients
11 (cc) and the relationships between v_A and $v-V_{HT}$ in each panel), five Walén tests resulted in very high
12 correlation coefficients with negative and nearly unity slopes, except for the failure at UT 19:06, possibly
13 because of the decrease in the ion density, as shown in Figure 2 panel 1. The time intervals and the results of
14 the Walén tests are listed in table 1. The negative slopes indicate that the spacecraft was located south of the
15 reconnection site. This is consistent with the observed southward and tailward directions of the accelerated
16 flows. The near unity values of the slopes indicate the agreement of the observed velocity with the Alfvénic
17 acceleration during the reconnection processes.
18

19 Furthermore, with accounting of the anisotropic pressure, the prediction of Alfvénic acceleration during the
20 reconnection was calculated and compared to the observed velocity. Based on a single point reference in the
21 magnetosheath and local magnetic field measurements, the flow prediction could be calculated as:
22 $\Delta \mathbf{v}_{\text{predicted}} = \mathbf{v}_{2t} - \mathbf{v}_{1t} = -(1-\alpha)^{1/2} (\mu_0 \rho_1)^{-1/2} [\mathbf{B}_{2t}(1-\alpha_2)/(1-\alpha_1)]$ (Hudson, 1970; Paschmann et al, 1986). The negative sign
23 was chosen from the observed negative correlation between $\Delta \mathbf{v}$ and $\Delta \mathbf{B}$ at the magnetopause. Subscript “1”
24 denotes the reference time at 19:07 UT and “2” denotes the prediction for every other time. The pressure
25 anisotropy factor is $\alpha = (p_{\parallel} - p_{\perp}) \mu_0 / B^2$. As illustrated in figure 4 panels 2 and 3, the predicted tangential V_x and V_z
26 were marked by red points only when the ion density was higher than 6 cm^{-3} (the black line in Panel 2 of
27 Figure 2). At the magnetopause current sheet crossings, the predicted V_x and V_z agree with observations quite
28 well. The observed low ion density at 19:06 UT could explain why the Walén test failed there. In the boundary
29 layer, there are still several predictions of the accelerated flows close to the observed velocity, with the ion
30 density higher than 6 cm^{-3} . The agreement of the predicted V_x and V_z with the observations in the
31 magnetopause current sheets is consistent with the results of the Walén tests. Both results indicate that the
32 observed fast flows were generated by reconnection which might be continuously active somewhere north of
33 the spacecraft. The medium ion density ($1 \text{ cm}^{-3} \sim 6 \text{ cm}^{-3}$) and temperature in the boundary layer and even
34 inside the magnetosphere (for a few hours not shown before 17:35 UT) indicate the mixture of the cold and
35 dense plasma from the magnetosheath with the hot and diluted plasma from the magnetosphere via the open
36 magnetic field line generated by reconnection.
37
38
39
40
41
42

43 3 Discussion

44 In the **presented** observations, there is no evidence for the spacecraft crossing the vicinity of the
45 reconnection site. In fact, the draped IMF observed by Cluster in the upstream magnetosheath in this event was
46 mainly dawnward ($-B_y$) and anti-sunward ($-B_x$), with $B_z \approx 0$ nT. According to the anti-parallel reconnection
47 model, when the IMF is dominantly dawnward, the reconnection site could be located at the northern high
48 latitude region at the dawnside and the southern high latitude at the duskside, as illustrated in Figure 5 (a). On
49 the other hand, the component reconnection site should be located as a tilted X-line from north-dawn quadrant
50 to south-dusk quadrant under dawnward IMF ($-B_y$) (Sonnerup et al, 1974, Gonzales and Mozer, 1974), as
51 illustrated in Figure 5(b). The reconnection site can be predicted to be north of the TC-1 position, whether the
52 reconnection was anti-parallel or component. This implies that the observed tailward ($-V_x$) and southward ($-V_z$)
53 fast flows should come from the reconnection site in the other hemisphere, far away from the spacecraft. The
54 direction of the accelerated flows is consistent with the expected location of either anti-parallel or component
55 reconnection. The magnetic shear angle across the magnetopause at TC-1 was about 62° , far from 180° .
56
57
58
59
60
61
62
63
64
65

1
2
3
4 However, we could not tell whether the reconnection was anti-parallel or component because the spacecraft
5 was far away from the reconnection site, but this event could be considered as supporting either of them.

6
7 Reconnection at the magnetopause can be quasi-steady (Paschmann et al 1979) or time-dependent (Russell
8 and Elphic, 1978). In Panel 4 of Figure 2, the fast flows lasted about one hour with some modulation of the
9 magnetopause motion. In the quasi-steady scenario, due to the motion of the magnetopause, the TC-1
10 encounters the reconnected fast flows at different distances from the magnetopause: when the magnetopause
11 moves inward, the TC-1 is closer to the magnetopause and encounters the more accelerated flows. On the other
12 hand, when the magnetopause moves outward, the TC-1 is located deeper inside the boundary layer, and
13 slower flows are observed. The repeated encounters of reconnection jets at multiple magnetopause crossings
14 could be considered as evidence for continuous reconnection (Gosling et al, 1982). During the one-hour
15 interval, nearly 80% of the time was filled by the fast flows, quite continuously even in the single spacecraft
16 observation. It implies that the reconnection might be active continuously during the interval. Figure 6 gives
17 the plot of $|V_{\parallel}|$ as a function of N_i , which is a good illustration that the reconnection was quasi-continuous
18 because the velocity in the multiple magnetopause/boundary layer crossings was mostly enhanced compared to
19 the magnetosheath velocity (Phan et al, 2004; Hasegawa et al, 2008). The acceleration was observed in the
20 boundary layer quite continuously, with only few low points between the ion density of $1-6 \text{ cm}^{-3}$ in the
21 boundary layer.

22
23 On the other hand, a series of FTEs can be seen during the quasi-continuous reconnection, marked by the
24 vertical lines in panels 5 and 6 of Figure 2. As mentioned above, these FTEs correspond to the intervals with
25 increases or decreases in the flow speed, indicating the passage of the reconnected flux tubes over the
26 spacecraft. However, the series of FTEs also showed some intermittency in themselves, implying that they
27 might also be caused by repeated plasmoids as suggested by Raeder (2006). If so, the intermittent FTEs can be
28 driven by quasi-continuous reconnection. There seems to be somehow mixed features in the observation. The
29 medium density ($1 \text{ cm}^{-3}-6 \text{ cm}^{-3}$) and temperature of the ions in the boundary layer and even deeper inside the
30 magnetosphere could indicate the entry of the cold and dense plasma from the magnetosheath. There was little
31 difference in the plasma β between the magnetosphere and magnetosheath, which also implies the entry of the
32 magnetosheath plasma into the magnetosphere. The presented observations show the quasi-continuous
33 reconnection accompanied by time-dependent FTEs when the draped IMF B_z was close to 0 nT, and can
34 support the existence of the extended reconnection process (Phan et al, 2000, 2001) that drives the plasma
35 transport into the magnetosphere at the dawnside magnetopause.
36
37
38
39

40 **4 Summary**

41
42 The reconnection at the magnetopause can be either steady or time-dependent. The TC-1 observed quasi-
43 continuous reconnection accompanied by FTEs when the draped IMF B_z was close to 0 nT in the event
44 presented in this paper. The conclusions of the analysis are summarized as follows:

45 (1) During the one-hour interval of IMF $B_z \approx 0$, reconnection jets were observed by TC-1 with velocities up
46 to more than 500 km/s at the south-dawn flank magnetopause, significantly higher than the background flows
47 in the magnetosheath.
48

49 (2) Walén tests at the magnetopause crossings indicate that the fast flows satisfied the Walén relation quite
50 well, and the observed velocity of the fast flows matched the theoretical prediction for Alfvénic acceleration
51 very well, indicating that the accelerated flows were generated by reconnection.
52

53 (3) The negative slopes of the Walén test showed that the spacecraft was located south of the reconnection
54 site, consistent with the observed southward and tailward flows, but the event could not be used to identify
55 whether the reconnection was anti-parallel or component.
56

57 (4) The reconnection was indicated to be quasi-continuously active at the magnetopause north of the
58 spacecraft, and it was simultaneously accompanied by a series of time-dependent FTEs, showing the features
59 of quasi-steadiness and time-dependence simultaneously.
60
61
62
63
64
65

1
2
3
4 (5) The presented observation could support the extension of the reconnection process to the flank
5 magnetopause; this process converts magnetic energy into plasma energy and causes solar wind transport into
6 the magnetosphere.
7
8
9

10 **Acknowledgement:**

11 This work was supported by the National Natural Science Foundation of China Grant No. 41004074,
12 41211120182, 41231066, 40774081, the Ministry of Science and Technology of China Grant
13 2011CB811404, the China Scholar Council Grand No. 201404910003, and the Specialized Research Fund
14 for State Key Laboratories of the CAS.
15
16
17
18

19 **References**

- 20 Balogh, A., Carr, C. M., Acuna, M. H., Dunlop, M. W., Beek, T. J., Brown, P., Fornaçon, K.-H., Georgescu, E.,
21 Glassmeier, K.-H., Harris, J., Musmann, G., Oddy, T., Schwingenschuh, K. The Cluster magnetic field investigation:
22 overview of in-flight performance and initial results. *Ann. Geophys.*, 19, 1207–1217, 2001.
- 23 Bogdanova, Y. V., Marchaudon, A., Owen, C. J., Dunlop, M. W., Frey, H. U., Wild, J. A., Fazakerley, A. N.,
24 Klecker, B., Davies, J. A., Milan, S. E. On the formation of the high-altitude stagnant cusp: Cluster observations.
25 *Geophys. Res. Lett.*, 32(12), L12101, DOI: 10.1029/2005GL022813, 2005.
- 26 Bogdanova, Y. V., Owen, C. J., Dunlop, M. W., Wild, J. A., Davies, J. A., Lahiff, A. D., Taylor, M. G. G. T.,
27 Fazakerley, A. N., Dandouras, I., Carr, C. M., Lucek, E. A., Rème, H. Formation of the low-latitude boundary layer
28 and cusp under the northward IMF: Simultaneous observations by Cluster and Double Star. *J. Geophys. Res.*,
29 113(A7), A07S07, DOI: 0.1029/2007JA012762, 2008
- 30 Carr, C., Brown, P., Zhang, T. L., Gloag, J., Horbury, T., Lucek E., Magnes, W., O'Brien, H., Oddy, T., Auster,
31 U., Austin, P., Aydogar, O., Balogh, A., Baumjohann, W., Beek, T., Eichelberger, H., Fornaçon, K.-H., Georgescu,
32 E., Glassmeier, K.-H., Ludlam, M., Nakamura, R., Richter, I. The Double Star magnetic field investigation:
33 instrument design, performance and highlights of the first year's observations. *Ann. Geophys.*, 23, 2713–2732, 2005.
- 34 Chandler, M. O., Fuselier, S. A., Lockwood, M., Moore, T. E. Evidence of the component merging equatorward
35 of the cusp. *J. Geophys. Res.*, 104(A10), 22623-22633, 1999.
- 36 Cowley, S. W. H. A quantitative study of the reconnection between the Earth's magnetic field and an
37 interplanetary field of arbitrary orientation. *Radio Sci.*, 8(11), 903-913, 1973.
- 38 Crooker, N. U. Dayside merging and cusp geometry. *J. Geophys. Res.*, 84(A3), 951-959, 1979.
- 39 Dungey, J. W. Interplanetary magnetic field and auroral zones. *Phys. Rev. Lett.*, 6(2), 47-48, 1961.
- 40 Dunlop, M. W., Taylor, M. G. G. T., Davies, J. A., Owen, C. J., Pitout, F., Fazakerley, A.N., Pu, Z., Laakso, H.,
41 Bogdanova, Y. V., Zong, Q.-G., Shen, C., Nykyri, K., Lavraud, B., Milan, S. E., Phan, T. D., Rème, H., Escoubet, C.
42 P., Carr, C. M., Cargill, P., Lockwood, M., Sonnerup, B. U. Ö., Coordinated Cluster/Double Star observations of
43 dayside reconnection signatures. *Ann. Geophys.*, 23(11), 2867-2875, 2005.
- 44 Dunlop, M. W., Zhang, Q. H., Xiao, C. J., He, J. S., Pu, Z., Fear, R. C., Shen, C., Escoubet, C. P. Reconnection at
45 high latitudes: anti-parallel merging. *Phys. Rev. Lett.* 102(7), 075005, 2009.
- 46 Frey, H. U., Phan, T. D., Fuselier, S. A., Mende, S. B. Continuous magnetic reconnection at Earth's
47 magnetopause. *Nature*, 626, 533-537, 2003.
- 48 Gonzales, W. D., Mozer, F. S. A quantitative model for the potential resulting from reconnection with an arbitrary
49 interplanetary magnetic field. *J. Geophys. Res.*, 79, 4186-4194, 1974.
- 50 Gosling, J. T., Asbridge, J. R., Bame, S. J., Feldman, W. C., Paschmann, G., Sckopke, N., Russell, C. T. Evidence
51 for quasi-stationary reconnection at the dayside magnetopause. *J. Geophys. Res.*, 87, 2147-2158, 1982.
- 52 Hasegawa, H., Retino, A., Vaivads, A., Khotyaintsev, Y., Nakamura, R., Takada, T., Miyashita, Y., Reme, H.,
53 Lucek, E. A. Retreat and reformation of X-line during quasi-continuous tailward-of-the-cusp reconnection under
54 northward IMF. *Geophys. Res. Lett.*, 35, L15104, doi:10.1029/2008GL034767, 2008.
55
56
57
58
59
60
61
62
63
64
65

- 1
2
3
4 Kan, J. R. A Theory of Patchy and Intermittent Reconnections for Magnetospheric Flux Transfer Events. *J.*
5 *Geophys. Res.*, 93(A6), 5613-5623, 1988.
- 6 Kan, J. R., Lyu, L. H., Deehr, C. S., Newell, P. T. Ionspheric signatures of patchy-intermittent reconnection at
7 dayside magnetopause, *J. Geophys. Res.*, 101(A5), 10939–10945, 1996.
- 8 Karimabadi, H., Daughton W., Quest, K. B. Anti-parallel versus component merging at the magnetopause:
9 Current bifurcation and intermittent reconnection. *J. Geophys. Res.*, 110, A03213, 2005.
- 10 Khrabrov, A. V. and Sonnerup, B. U. Ö. deHofmann-Teller Analysis, *Analysis Methods for Multi-Spacecraft*
11 *Data*, edited by: Paschmann G. and P. W. Daly, ISSI Science Report, SR-001, 221–248, 1998.
- 12 Kim, K.-H., Lin, N., Cattell, C. A., Song, Y., Lee, D.-H. Evidence for component merging near the subsolar
13 magnetopause: Geotail observations. *Geophys. Res. Lett.*, 29(6), 1080-1082, doi: 10.1029/2001GL014636, 2002..
- 14 Liu, Z. X., Escoubet, C. P., Pu, Z. Y. Laakso, H., Shi, J. K., Shen, C., Hapgood, M. The Double Star mission. *Ann.*
15 *Geophys.*, 23, 2707-2712, 2005.
- 16 Luhmann, J. G., Walker, R. J., Russell, C. T., Crooker, N. U., Spreiter, J. R., Stahara, S. S. Patterns of potential
17 magnetic field merging sites on the dayside magnetopause. *J. Geophys. Res.*, 89, 1739-1742, 1984.
- 18 Paschmann, G., Sonnerup, B. U. Ö., Papamastorakis, I., Sckopke, N., Haerendel, G., Bame, S. J., Asbridge, J. R.,
19 Gosling, J. T., Russell, C. T., Elphic, R. C. Plasma acceleration at the earth's magnetopause. Evidence for
20 reconnection, *Nature*, 282, 243–246, 1979.
- 21 Phan, T. D., Kistler, L. M., Klecker, B., Haerendel, G., Paschmann, G., Sonnerup, B. U. Ö., Baumjohann, W.,
22 Bavassano-Cattaneo, M. B., Carlson, C. W. DiLellis, A. M., Fornacon, K.-H, Frank, L. A., Fujimoto, M., Georgescu,
23 E., Kokubun, S., Moebius, E., Mukai, T., Øieroset, M., Paterson, W. R., Rème, H. Extended magnetic reconnection
24 at the Earth's magnetopause from detection of bi-directional jets. *Nature*, 404, 848–850, 2000.
- 25 Phan, T. D., Freeman, M. P., Kistler, L. M., Klecker, B., Haerendel, G., Paschmann, G., Sonnerup, B. U. Ö.,
26 Baumjohann, W., Bavassano-Cattaneo, M. B., Carlson, C. W. DiLellis, A. M., Fornacon, K.-H, Frank, L. A.,
27 Fujimoto, M., Georgescu, E., Kokubun, S., Moebius, E., Mukai, T., Paterson, W. R., Rème, H. Evidence for an
28 extended reconnection line at the dayside magnetopause, *Earth Planet Space*, 53, 619–625, 2001.
- 29 Phan, T. D., M. W. Dunlop, G. Paschmann, B. Klecker, J. M. Bosqued, H. Rème, A. Balogh, C. Twitty, F. S.
30 Mozer, C. W. Carlson, C. Mouikis, and L. M. Kistler: Cluster observations of continuous reconnection at the
31 magnetopause under steady interplanetary magnetic field conditions, *Ann. Geophys.*, 22, 2355-2367, 2004.
- 32 Phan, T. D., Hasegawa, H., Fujimoto, M., Øieroset, M., Mukai, T., Lin, R. P., Paterson, W. Simultaneous Geotail
33 and Wind observations of reconnection at the subsolar and tail flank magnetopause. *Geophys. Res. Lett.*, 33(9),
34 L09104, doi:10.1029/2006GL025756, 2006..
- 35 Pu, Z. Y, Xiao, C. J., Zhang, X. G., Huang, Z. Y., Fu, S. Y., Liu, Z. X., Dunlop, M. W., Zong, Q. G., Carr, C. M.,
36 Rème, H., Dandouras, I., Fazakerley, A., Phan, T. D., Zhang, T. L., H. Zhang, Wang, X. G. Double Star TC-1
37 observations of component reconnection at the dayside magnetopause. *Ann. Geophys.*, 23(11), 2889-2895, 2005.
- 38 Quest, K. B., Coroniti, F. V. Tearing at the dayside magnetopause, *J. Geophys. Res.*, 86, 3289-3298, 1981.
- 39 Raeder, J. Flux Transfer Events: 1. generation mechanism for strong southward IMF, *Ann. Geophys.*, 24, 381-392,
40 2006.
- 41 Rème, H., Dandouras I., Aoustin, C. Bosqued, J. M., Sauvaud, J. A., Vallat, C., Escoubet, C. P., Cao, J. B., Shi, J.
42 K., Bacassano-Cattaneo, M. B., Parks, G. K., Carlson, C. W., Pu, Z. Y., Klecker, B., Moebius, E., Kistler, L., Korth,
43 A., Lundin, R. The HIA instrument onboard the Tan Ce 1 Double Star near-Equatorial Spacecraft and its first results,
44 *Ann. Geophys.*, 23, 2757-2774, 2005.
- 45 Rosenqvist L., Vaivads, A., Retino, A., Phan, T. D., Opgenoorth, H. J., Dandouras, I., Buchert, S. Modulated
46 reconnection rate and energy conversion at the magnetopause under steady IMF conditions, *Geophys. Res. Lett.*, 35,
47 L08104, doi:10.1029/2007GL032868, 2008.
- 48 Russell, C. T, Elphic, R. C. Initial ISEE Magnetometer Results: Magnetopause Observations, *Space Sci. Rev.*, 22,
49 681-715, 1978.
- 50 Russell, C. T, Elphic, R. C. ISEE observations of Flux Transfer Events at the Dayside Magnetopause, *Geophys.*
51 *Res. Lett.*, 6, 33-36, 1979.
- 52
53
54
55
56
57
58
59
60
61
62
63
64
65

1
2
3
4 Song, P., Russell, C. T. Model of the formation of the low-latitude boundary layer for strongly northward
5 interplanetary magnetic field. *J. Geophys. Res.*, 97(A2), 1411-1420, 1992.
6 Sonnerup, B. U. Ö. Magnetopause reconnection rate. *J. Geophys. Res.*, 79, 1546-1549, 1974.
7 Sonnerup, B. U. Ö. On the stress balance in flux transfer events. *J. Geophys. Res.*, 92, 8613-8620, 1987.
8 Trattner, K. J., Mulcock, J. S., Petrinec, S. M., Fuselier, S. A. Probing the boundary between anti-parallel and
9 component reconnection during southward interplanetary magnetic field conditions. *J. Geophys. Res.*, 112, A08210,
10 2007.
11 Yan, G. Q., Shen, C., Liu, Z. X., Rème, H., Dunlop, M. W., Lucek, E., Carr, C. M., Zhang T. L. Solar wind
12 transport into magnetosphere caused by magnetic reconnection at high latitude magnetopause during northward IMF:
13 Cluster-DSP conjunction observations. *Sci in China (E)*, 51(10), 1677-1684, 2008.
14 Yan, G. Q., Liu, Z. X., Shen, C., M. W. Dunlop, Luseck, E., Rème, H., Bogdanova Y. V., Fazakerley, A. Solar
15 wind entry via flux tube into magnetosphere observed by Cluster measurements at dayside magnetopause during
16 southward IMF. *Sci. in China (E)*, 52(7), 2104-2111, 2009.
17 Zong, Q. G., Bhattacharjee, A. Plasmoid in the high latitude boundary/cusp region observed by Cluster. *Geophys.*
18 *Res. Lett.*, 32, L01101, 2005. doi: 10.1029/2004GL020960.
19 Zhang, H., Kivelson, M. G., Khurana, K. K., Walker, R. J., Angelopoulos, V., Phan, T., McFadden, J., Larson,
20 D., Glassmeier, K. H., Auster H. U. Evidence that crater flux transfer events are initial stages of typical flux transfer
21 events. *J. Geophys. Res.*, 115, A08229, 2010. doi:10.1029/2009FA015013.
22
23
24
25
26
27
28
29
30
31
32
33
34
35
36
37
38
39
40
41
42
43
44
45
46
47
48
49
50
51
52
53
54
55
56
57
58
59
60
61
62
63
64
65

1
2
3
4
5
6
7
8
9
10
11
12
13
14
15
16
17
18
19
20
21
22
23
24
25
26
27
28
29
30
31
32
33
34
35
36
37
38
39
40
41
42
43
44
45
46
47
48
49
50
51
52
53
54
55
56
57
58
59
60
61
62
63
64
65

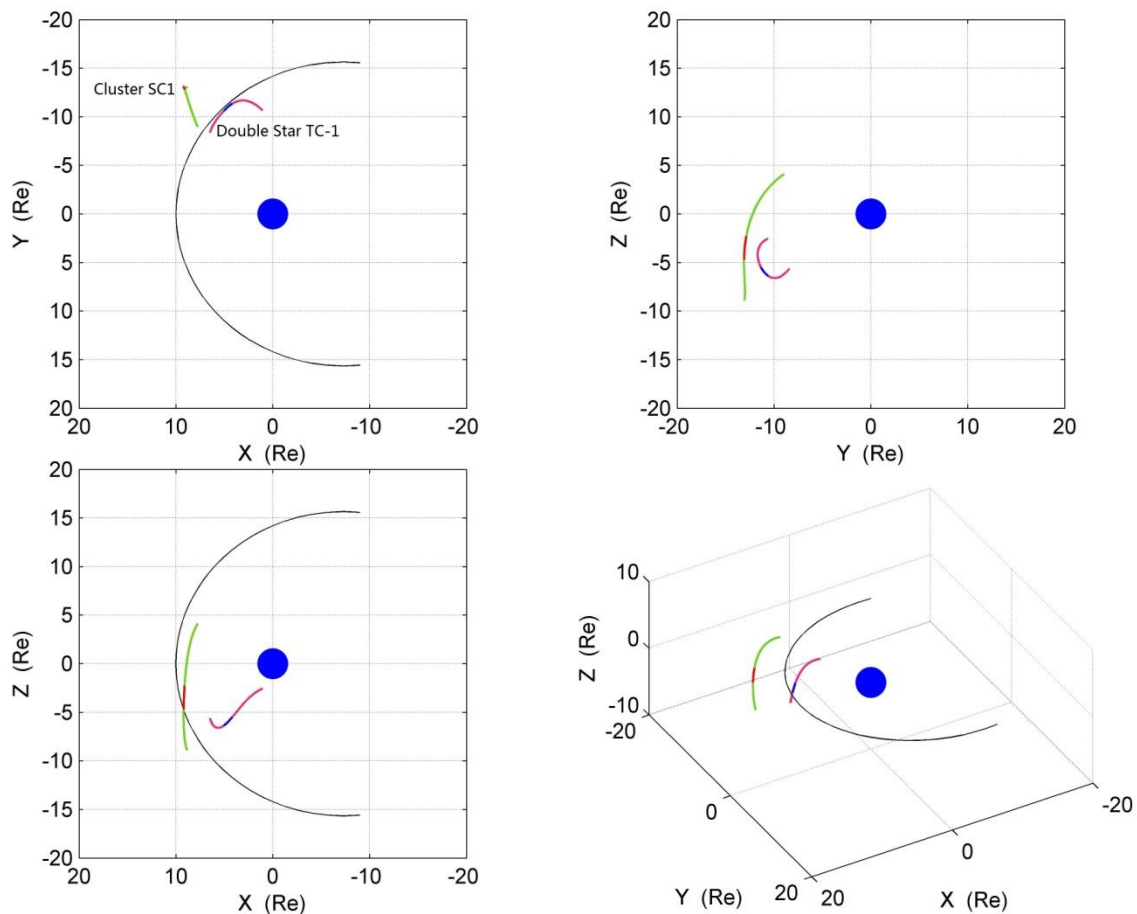


Figure 1. Orbits of the Double Star TC-1 near the magnetopause and Cluster SC1 in the upstream magnetosheath, with similar magnetic local time during the interval of interest. The relative position of the TC-1 and SC1 orbits and the magnetopause are shown in the X-Y plane (top left panel), the X-Z plane (bottom left panel), and the Y-Z plane (top right panel) and in 3D (bottom right panel). The investigated interval is marked by the blue color for TC1 and by the red for SC1. The position vectors are presented in GSM coordinates.

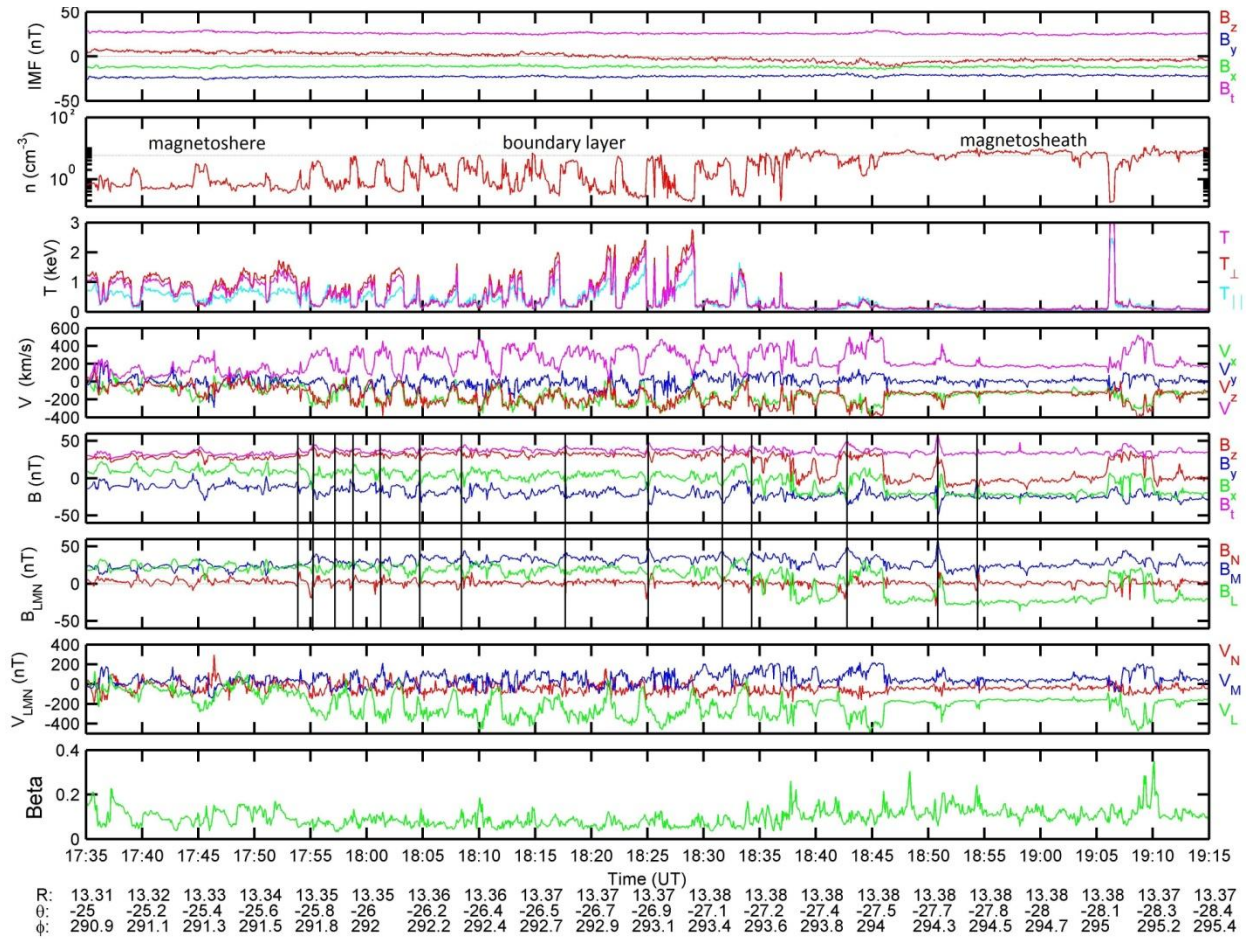


Figure 2. TC-1 observations at the south-dawn flank of the magnetopause and the IMF monitored by the Cluster SC1 in the upstream magnetosheath. Panel 1 indicates the IMF in GSM coordinates observed by Cluster SC1 in the upstream magnetosheath, with the time lag of 2 minutes from SC1 to TC1 counted. Panel 2 shows the ion density in logarithmic coordinate; panel 3 presents the ion temperature; panel 4 and 7 show the ion bulk velocity in GSM coordinates and in boundary coordinates, respectively; panel 5 and 6 present the magnetic field in GSM coordinates and in boundary coordinates, respectively; and panel 8 shows the plasma β . The boundary coordinates were calculated by the minimum variation analysis (MVA) method at the magnetopause crossing, L was northward and tailward, M was downward, and N outward normal to the magnetopause.

1
2
3
4
5
6
7
8
9
10
11
12
13
14
15
16
17
18
19
20
21
22
23
24
25
26
27
28
29
30
31
32
33
34
35
36
37
38
39
40
41
42
43
44
45
46
47
48
49
50
51
52
53
54
55
56
57
58
59
60
61
62
63
64
65

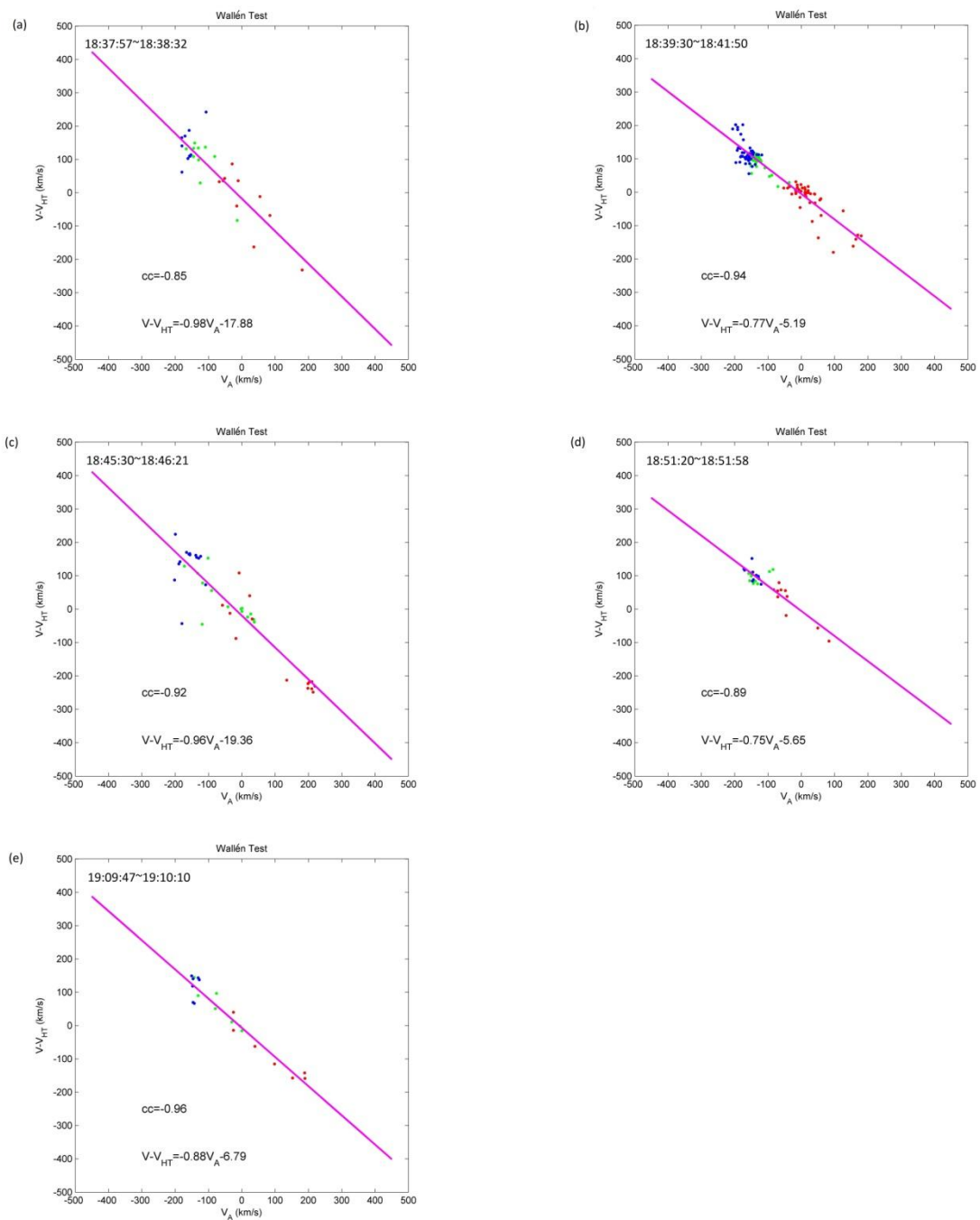


Figure 3. Walén test plots of $V - V_{HT}$ vs V_A at the magnetopause current sheet crossings. The time intervals, correlations coefficients (cc) and the relationships between v_A and $v - V_{HT}$ were presented in each panel. Five tests result in high correlation coefficients, negative and nearly unity slopes of the Walén relations. The V_x , V_y , V_z were plotted as data points in green, blue and red, respectively. The panel a-e correspond to the intervals number 1, 2, 3, 4, and 6 in Table 1.

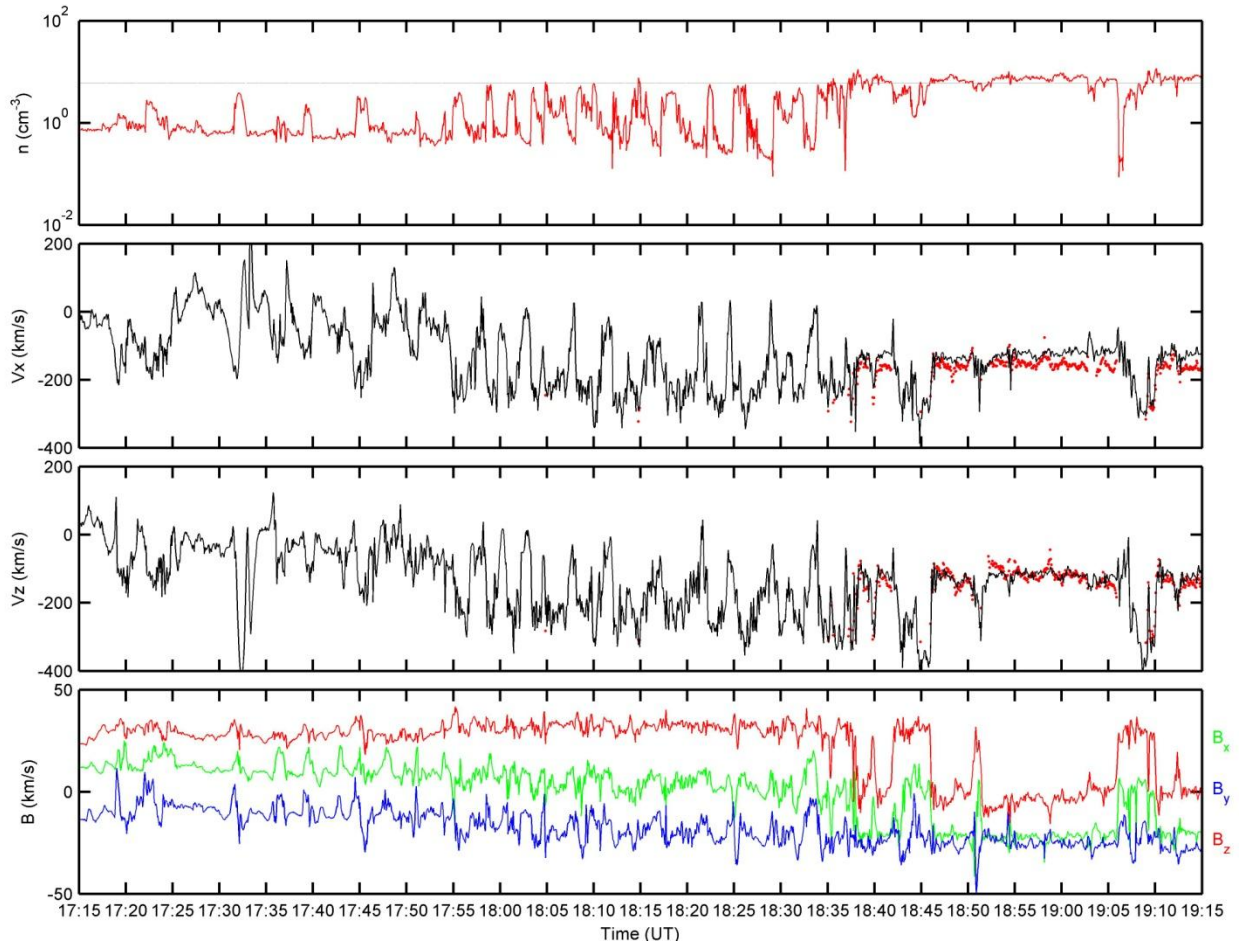


Figure 4. Comparison of the predicted V_x and V_z to the observed velocity. Panel 1 gives the ion density observed by HIA, the straight line in black is the level of 6 cm^{-3} ; Panel 2 presents the observed V_x as a black line and the predicted V_x as red dots; Panel 3 indicated the observed V_z as a black line and the predicted V_z as red dots; Panel 4 shows the observed magnetic field measured by TC-1 FGM.

1
2
3
4
5
6
7
8
9
10
11
12
13
14
15
16
17
18
19
20
21
22
23
24
25
26
27
28
29
30
31
32
33
34
35
36
37
38
39
40
41
42
43
44
45
46
47
48
49
50
51
52
53
54
55
56
57
58
59
60
61
62
63
64
65

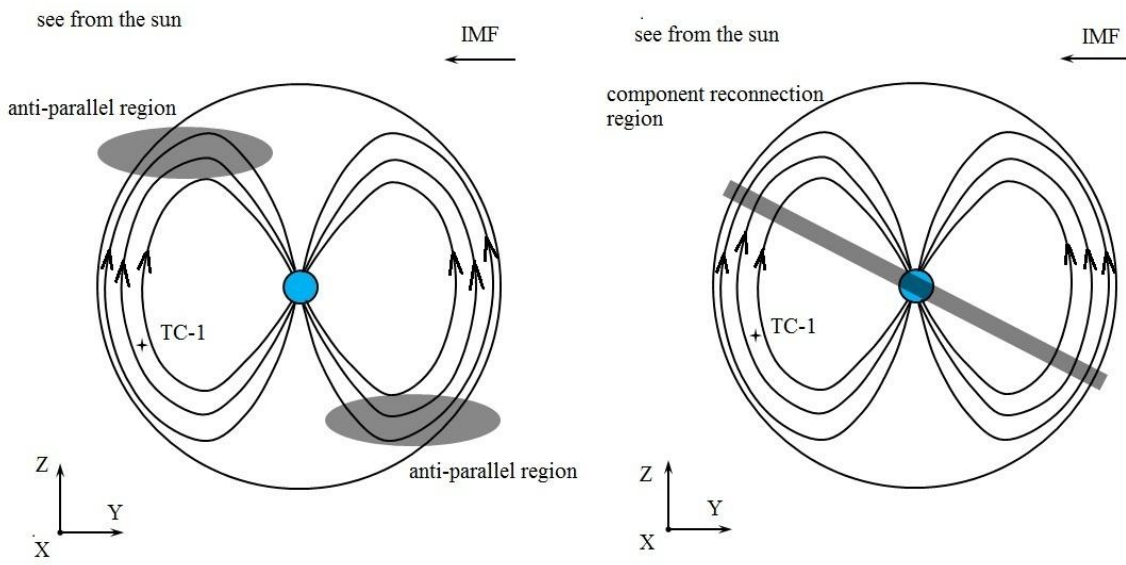


Figure 5. (a) Illustration of the location of the anti-parallel reconnection region under the IMF of $B_z \approx 0$ nT; (b) Illustration of the location of the component reconnection region under the same IMF condition.

1
2
3
4
5
6
7
8
9
10
11
12
13
14
15
16
17
18
19
20
21
22
23
24
25
26
27
28
29
30
31
32
33
34
35
36
37
38
39
40
41
42
43
44
45
46
47
48
49
50
51
52
53
54
55
56
57
58
59
60
61
62
63
64
65

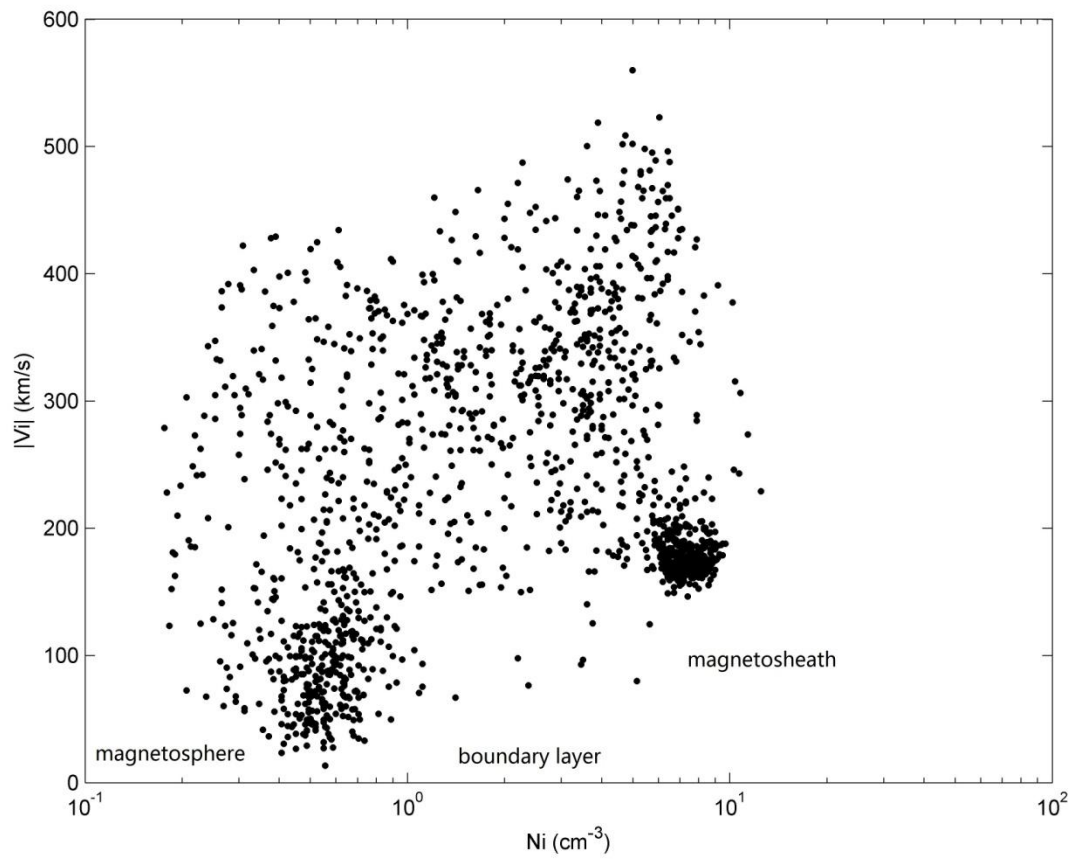


Figure 6 Scatter plot of the ion velocity as a function of ion number density for the interval. The flows in the boundary layer are enhanced relative to the magnetosheath flows at most of the measured points.

Table 1. Walén test results at the magnetopause current sheet crossings. The numbers of the crossings are in the first column. The time intervals of the magnetopause crossings are in the second column. The correlation coefficients between $V-V_{HT}$ and V_A at every crossing are presented in the third column. The slopes of the Walén relationships are in the fourth column, and the fifth column gives the V_{HT} .

NUM	time interval (UT)	cc	slope	V_{HT}
1	18:37:57~18:38:32	-0.85	-0.98	[-268.77, -153.85, -140.30]
2	18:39:30~18:41:50	-0.94	-0.77	[-231.33, -117.93, -120.60]
3	18:45:30~18:46:21	-0.92	-0.96	[-259.05, -76.72, -141.18]
4	18:51:20~18:51:58	-0.89	-0.75	[-261.10, -94.78, -206.55]
5	19:06:21~19:07:43	-0.29	-0.09	test failed
6	19:09:47~19:10:10	-0.96	-0.88	[-258.01, -71.60, -170.98]